9(2012) 353 – 365

Latin American Journal of Solids and Structures

www.lajss.org

Buckling analysis of laminated composite plates using an efficient C^0 FE model

Abstract

Buckling analysis of laminated composite plates is carried out by using an efficient C^0 FE model developed based on higher order zigzag theory. In this model the first derivatives of transverse displacement have been treated as independent variables to overcome the problem of C^1 continuity associated with the FE implementation of the plate theory. The C^0 continuity of the present FE model is compensated in the stiffness matrix calculations by using penalty parameter approach. Numerical results and comparison with other existing solutions show that the present model is very efficient in predicting the buckling responses of laminated composites.

Keywords

Buckling, laminated composites, Finite element analysis

S. K. Singh* **and A. Chakrabarti**

Department of Civil Engineering, Indian Institute of Technology, Roorkee-247 667, India
Ph.+91(1332)285844, Fax.+91(1332)275568

Received 10 Apr 2012;
In revised form 23 Apr 2012

* Author email: sushilbit@yahoo.co.in

1 INTRODUCTION

Laminated composite plates are widely used in civil infrastructure systems due to their high strength to weight ratio and flexibility in design. One of the main failure mechanisms in composite plates is buckling. Accurate prediction of structural response characteristics is a challenging problem in the analysis of laminated composites due to the orthotropic structural behavior, the presence of various types of couplings and due to less thickness of the structural elements made of composites. Thus, an accurate buckling analysis of the laminated composite plates is an important part of the structural design.

Finite element method has been widely used for the buckling analysis of laminated composite plates. To predict the buckling load of composite plates, a number of plate theories have been proposed. The classical laminate plate theory (CLPT), which neglects the transverse shear deformation effect, yields acceptable results only for thin laminates[32]. The structures designed based on CLPT theory may be unsafe because the CLPT overestimates the buckling load of the laminated composite plates. To take into account the effect of transverse shear deformation, the first-order shear deformation theory (FSDT)[1, 28] has been used to predict the dynamic response of laminated composite structures. In the first-order shear deformation theory (FSDT) a shear correction factor is used to compensate for the assumed uniform transverse shear strain variations over the entire plate thickness. For a better representation

of the transverse shear deformations, various higher-order shear deformation (HSDT) plate theories[5, 15, 16, 30, 36] were proposed. However, it has been observed and mentioned by many researchers[3] that increasing the number of terms in the in-plane displacement components does not improve the results and it is required to add the effect of inter-laminar transverse shear stress continuity in a multilayered composite plate problem.

A major development in this direction is due to Di Sciuva[34], Murakami[23], Liu et al.[20], and few others. They proposed zigzag plate theory where layer-wise theory is initially used to represent the in-plane displacements having piecewise linear variation across the thickness. The unknowns at the different interfaces are subsequently expressed in terms of those at the reference plane through satisfaction of transverse shear stress continuity at the layer interfaces. This theory is known as refined first order shear deformation theory (RFSDT). A further improvement in this direction is due to Di Sciuva [35], Bhaskar et al.[2], Cho et al.[8, 16] and some other investigators. They included the condition of zero transverse shear stress at top and bottom of the plate in addition to the shear stress free conditions at the layer interfaces. This theory is known as higher order zigzag theory (HZT) or refined higher order shear deformation theory.

However, all these refined theories including the HSDT demand C^1 continuity of the transverse displacement along the element edges at the time of their finite element implementation. However, a C^1formulation is not encouraged in any practical applications. In this situation it is highly required to develop a C^0 finite element formulation which will overcome the above C^1continuity requirement of the theory (HZT).

Typically most of the C^0 refined theories[18, 19, 40] en-force the mentioned continuity assuming the displacement and transverse stresses as primary variable for multilayered composite plates employing the FE method and showed a good agreement with three dimensional elasticity solutions. On the other hand Ferreira et al. [39] combined the third order theory of Reddy[11] with a meshfree method based on the multi-quadric radial basis function approach to study the behavior of multilayered laminated composite beams and plates. Mondal et al. [29] analyzed the elastic stability behavior of simply supported anisotropic sandwich flat panels subjected to mechanical in-plane loads by using an analytical approach. Shufrin et al.[22] used a semi analytical approach for the buckling analysis of symmetrically laminated rectangular plates with general boundary conditions. Ganapathi et al.[37] investigated the free vibration characteristics of simply supported anisotropic composite laminates using analytical approach. Nali et al.[14] analyzed buckling behaviour of laminated plates subjected to combined biaxial/shear loading. Ferriera et al.[24] used meshfree method based on collocation with radial basis functions for buckling and vibration analysis of laminated composite plates. Ferriera et al.[12] used numerical method for the buckling analysis of laminated plates based on collocation with wavelets. Nguyen-Van et al. [10] presented buckling and vibration analysis of composite plate or shell structures of various shapes. Fiedler et al.[25] used refined higher-order shear deformation theory for buckling analysis of multi-layered plates subjected to unidirectional in-plane loads. Moreover, it has been also observed that in some cases the violation of inter-laminar shear stress continuity might lead to higher buckling load.

In view of the above an efficient C^0 FE model has been developed based on a higher order zigzag theory (HZT) has been used to accurately predict the buckling load of laminated composite plates. The C^0continuity of the present finite element model has been compensated in the stiffness matrix formulation by using penalty parameter approach. A nine noded C^0 continuous isoparametric finite element has been used for the development of the proposed finite element model. To assess the accuracy, numerical results obtained by using the proposed finite element model based on HZT have been compared with the results of 3D elasticity, exact and other finite element solutions available in the literature.

2 FORMULATION

The in-plane displacement fields (Figure 1) are taken as below:

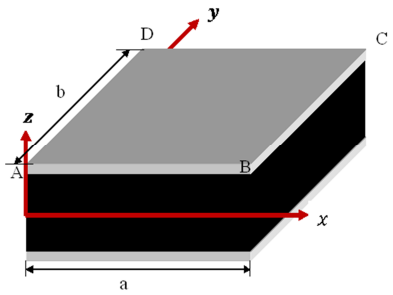

Figure 1 Geometry of laminated composite plate

$$u_\alpha = u_\alpha^0 + \sum_{k=0}^{nu-1} s_\alpha^k \left(Z - Z_k\right) H\left(Z - Z_k\right) + \sum_{k=0}^{nl-1} T_\alpha^k \left(Z - \rho_k\right) H\left(-Z + \rho_k\right) + \xi_\alpha Z^2 + \varphi_\alpha Z^3 \qquad (1)$$

where u_α^0 denotes the in-plane displacement of any point on the mid plane, n_u and $n_l$represent number of upper and lower layers respectively, S_α^k, T_α^k are the slopes of k-th layer corresponding to the upper and lower layers. $\xi_\alpha, \varphi_\alpha$ are the higher order unknown terms, $H(Z-Z_k), H(Z-P_k)$ are unit step functions and the subscript α represents the co-ordinate directions [α=1, 2 i.e. x, y in this case] respectively and

$$u_3 = w_0(x, y) \qquad (2)$$

The stres–sstrain relationship of a lamina, say k-th lamina having any fiber orientation with respect to the structural axes system (x-y-z) may be expressed as:

$$\bar{\sigma} = [\bar{Q}_k]\{\bar{\varepsilon}\} \qquad (3)$$

The rigidity matrix $\bar{Q}_k$ can be evaluated by material properties and fibre orientation following usual techniques followed in case of laminated composites and $\{\bar{\varepsilon}\}$ is the strain field vector of size (5×1) at the reference plane (i.e., at the mid plane).

Now by utilizing the transverse shear stress free boundary conditions ($\sigma_3\alpha|z = \pm h/2 = 0$) at the top and bottom surface of the plate the components ξ_α and φ_α may be expressed as:

$$\Phi_\alpha = -\frac{4}{3h^2}\left\{w_{,\alpha} + \frac{1}{2}\left(\sum_{k=0}^{nu-1} S_\alpha^K + \sum_{k=0}^{n_{l-1}} T_\alpha^k\right)\right\} \tag{4}$$

and

$$\xi_\alpha = -\frac{1}{2h}\left(\sum_{k=0}^{nu-1} S_\alpha^k - \sum_{k=0}^{nl-1} T_\alpha^k\right) \tag{5}$$

Similarly by imposing the transverse shear stress continuity conditions at the layer interfaces the following expressions for and are obtained:

$$S_\alpha^k = a_{\alpha\gamma}^k(w_{,\gamma} + \Psi_\gamma) + b_{\alpha\gamma}^k\, w,\gamma \tag{6}$$

$$T_\alpha^k = c_{\alpha\gamma}^k(w_{,\gamma} + \Psi_\gamma) + d_{\alpha\gamma}^k\, w,\gamma \tag{7}$$

where, $a_{\alpha\gamma}^k, b_{\alpha\gamma}^k, c_{\alpha\gamma}^k, d_{\alpha\gamma}^k$, are constants depending on material and geometric properties of individual layers,$W_{,\gamma}$ is the derivatives of transverse displacement while $\gamma = 1, 2$ and $S_\alpha^0 = \psi_\alpha$ is the rotation of normal at the mid plane about co-ordinate directions [α =1, 2 i.e., x, y in this case].

By using equations (2 -7) the strain field vector can be evaluated as below,

$$\{\bar{\varepsilon}\} = [H]\,\{\varepsilon\} \tag{8}$$

where $\{\varepsilon\}$ is the strain vector of size (17×1) at the reference plane (i.e., at the mid plane) where is the matrix of size (5×17) containing $z$terms and some terms related to material properties.

$$\{\varepsilon\}^T = \left\{ \begin{array}{cccccccccc} \frac{\partial u_1^0}{\partial x} & \frac{\partial u_2^0}{\partial y} & \frac{\partial u_2^0}{\partial x} + \frac{\partial u_1^0}{\partial y} & \frac{\partial w_1}{\partial x} & \frac{\partial w_2}{\partial y} & \frac{\partial w_2}{\partial x} & \frac{\partial w_1}{\partial y} & \frac{\partial \Psi_1}{\partial x} & \frac{\partial \Psi_2}{\partial y} & \\ \frac{\partial \Psi_2}{\partial x} & \frac{\partial \Psi_1}{\partial y} & \Psi_1 & \Psi_2 & \frac{\partial w}{\partial x} & \frac{\partial w}{\partial y} & w_1 & w_2 & & \end{array} \right\} \tag{9}$$

In present formulation based on higher order zigzag theory the in-plane displacement fields require C^1 continuity of the transverse displacement for its finite element implementation. In order to avoid the difficulties associated withC^1continuity, the derivatives of w with respect to x and y are expressed as follows.

$$\frac{\partial w}{\partial x} = w_1 \;\; and \;\; \frac{\partial w}{\partial y} = w_2 \tag{10}$$

which helps to define all the variables including and as C^0 continuous.

For the present study, a nine noded C^0 continuous isoparametric element shown in Figure 2 with seven nodal unknowns per node$(u_1, u_2, w, \Psi_1, \Psi_2, w_1, w_2)$ are used to develop the finite element formulation. The generalized displacements included in the present theory can be expressed as follows.

$$u_1 = \sum_{i=1}^{9} N_i u_i u_2 = \sum_{i=1}^{9} N_i v_i, u_3 = \sum_{i=1}^{9} N_i u_i, \Psi_1 = \sum_{i=1}^{9} N_i \Psi_{1_i},$$
$$\Psi_2 = \sum_{i=1}^{9} N_i \Psi_{2_i} \quad w_1 = \sum_{i=1}^{9} N_i w_{1_i} \quad w_2 = \sum_{i=1}^{9} N_i w_{2_i} \tag{11}$$

where N_i is the shape function for the nine noded isoparametric element[33].

Employing Hamilton's principle, the dynamic equation of equilibrium for a finite element can be formed. Accordingly the element stiffness matrix can be written as below

$$[K^e] = \sum_{i=1}^{nu+nl} \iiint [B]^T [H]^T [\bar{Q}^i] [H][B] dxdydz = \sum_{i=1}^{nu+nl} [B]^T [D] [B] dxdy \tag{12}$$

in which B is the strain matrix and Q^i is the transformed material constant matrix. where

$[D] = \sum_{k=1}^{n} \int [H]^T [\bar{Q}^i][H] dz$

In a similar manner the geometric strain vector may be expressed as,

$$\{\varepsilon_G\} = \begin{bmatrix} \frac{1}{2}\left(\frac{\partial \bar{w}}{\partial x}\right)^2 + \frac{1}{2}\left(\frac{\partial \bar{u}}{\partial x}\right)^2 + \frac{1}{2}\left(\frac{\partial \bar{v}}{\partial x}\right)^2 \\ \frac{1}{2}\left(\frac{\partial \bar{w}}{\partial y}\right)^2 + \frac{1}{2}\left(\frac{\partial \bar{u}}{\partial y}\right)^2 + \frac{1}{2}\left(\frac{\partial \bar{v}}{\partial y}\right)^2 \\ \left(\frac{\partial \bar{w}}{\partial x}\right)\left(\frac{\partial \bar{w}}{\partial y}\right) + \left(\frac{\partial \bar{u}}{\partial x}\right)\left(\frac{\partial \bar{u}}{\partial y}\right) + \left(\frac{\partial \bar{v}}{\partial x}\right)\left(\frac{\partial \bar{v}}{\partial y}\right) \end{bmatrix} = \frac{1}{2} \begin{bmatrix} \frac{\partial \bar{w}}{\partial x} & 0 & \frac{\partial \bar{u}}{\partial x} & 0 & \frac{\partial \bar{v}}{\partial x} & 0 \\ 0 & \frac{\partial \bar{w}}{\partial y} & 0 & \frac{\partial \bar{u}}{\partial y} & 0 & \frac{\partial \bar{v}}{\partial y} \\ \frac{\partial \bar{w}}{\partial y} & \frac{\partial \bar{w}}{\partial x} & \frac{\partial \bar{u}}{\partial y} & \frac{\partial \bar{u}}{\partial x} & \frac{\partial \bar{v}}{\partial y} & \frac{\partial \bar{v}}{\partial x} \end{bmatrix} \begin{Bmatrix} \frac{\partial \bar{w}}{\partial x} \\ \frac{\partial \bar{w}}{\partial y} \\ \frac{\partial \bar{u}}{\partial x} \\ \frac{\partial \bar{u}}{\partial y} \\ \frac{\partial \bar{v}}{\partial x} \\ \frac{\partial \bar{v}}{\partial y} \end{Bmatrix} \tag{13}$$

$$= \frac{1}{2}[A_G][\theta] = \frac{1}{2}[A_G][G][\Delta] \tag{14}$$

With the matrix [G] in the above equation, the geometric stiffness matrix of an element can be derived and may be written as

$$[k_g] = \sum_{i=1}^{nu+nl} \iiint [G]^T [S^k][G] dxdydz \tag{15}$$

where $[S^k]$ is the in-plane stress components of the k-th layer

Combining all the element geometric and elastic stiffness matrices, the dynamic equilibrium equation can be written as

$$([K] - \lambda [K_G]) \{\partial\} = 0) \tag{16}$$

in which $[K]$ and $[K_G]$ are the global elastic and geometric stiffness matrix, where$[\partial]$ is the mode shape vector of buckling and λ is the critical buckling load parameter respectively.

3 RESULTS AND DISCUSSION

In this section some problems on buckling of laminated composite plates are solved using the present finite element model considering different features such as boundary conditions, ply orientations, thickness ratio and aspect ratio. The results obtained by using the proposed FE model based on HZT is first validated with some published results and then many new results are also generated.

3.1 Simply supported square isotropic plates

In this example simply supported square isotropic (ν= 0.3) plate subjected to uni-axial loading is considered. The analysis is carried out for different thickness ratio (a/h = 100, 10). The critical buckling load obtained by using present FE model obtained are presented with the results of Chakrabarti and Sheikh [6] based on refined higher order shear deformation theory (RFSDT), Sundaresan et al. [38] based on first order shear deformation theory and that of general purpose finite element program MARC [38] in Table 1. It is observed that the present results are somewhat lesser than Chakrabarti and Sheikh [6], Sundaresan et al. [38] and general purpose finite element program MARC [38]. It may be due to efficient modeling of the transverse shear deformation followed in the present finite element model.

Table 1 Normalized Critical buckling loads (λ_{cr}) for square isotropic plate

Loading	a/h	References	λ_{cr}
uni-axial	100	Present(12×12^1)	
		Chakrabarti and Sheikh [6]	4.0
		Sundersan et al. [38]	4.0
		MARC [38]	4.0
	10	Present(12×12^1)	3.768
		Chakrabarti and Sheikh [6]	3.782

$$\lambda cr = \lambda \frac{a^2}{\pi^2 D} \; 1 - Meshdivision$$

3.2 Cross-ply multilayered (0/90/..) composite plate simply supported at all the edges

In this example the buckling of a laminated (0°/90°/90°/0°) square composite plate is considered. The material properties of the individual layers are given by: E_1/E_2 = open, $G_{12} = G_{13} = 0.6E_2$, $G_{23} = 0.5E_2$, $\nu_{12} = \nu_{13} = 0.25$.

This problem is solved to assess the performance of the proposed C^0 finite element model. The convergence and comparison of the normalized uni-axial critical buckling load obtained by using the proposed element is shown in Table 2. The thickness ratio (a/h) is varied (100 to 5) to cover the range of very thin to thick plates. It is found that with refining meshes, results obtained by the present FE model converge closely to the exact solution [26] and reasonably close to the 3D elasticity solution given by Noor [13]. The present finite element model based on higher order zigzag theory gives the more accurate results compared to the results given by

Fiedler et al. [33] based on a similar theory, results of Van et al. [25] based on first order shear deformation theory and results of Ferreira et al. [10] based on first order shear deformation theory respectively. Some new results are also presented in Table 2.

Table 2 Normalized critical uni-axial buckling loads (λ_{cr}) with various modular ratios for simply supported cross-ply [$0^0/90^0//90^0/0^0$] square plate

a/h	References	E_1/E_2				
		3	10	20	30	40
100	Present(2×2^1)	6.434	13.363	23.213	6.350	42.675
	Present(4×4)	5.855	11.837	20.331	5.781	37.118
	Present(6×6)	5.755	11.572	19.848	5.683	36.268
	Present(8×8)	5.721	11.486	19.702	5.650	36.039
	Present(12×12)	5.698	11.432	19.619	5.627	35.923
	Present(16×16)	5.690	11.417	19.599	5.619	35.898
	Fiedler et al. [13]	-	-	-	-	35.946
10	Present(2×2^1)	5.705	10.441	15.882	20.297	23.991
	Present(4×4)	5.297	9.810	15.143	19.516	23.191
	Present(6×6)	5.265	9.771	15.095	19.465	23.147
	Present(8×8)	5.259	9.764	15.091	19.465	23.138
	Present(12×12)	5.256	9.762	15.090	19.461	23.134
	Present(16×16)	5.256	9.761	15.064	19.460	23.133
	3-D Elasticity [26]	5.294	9.762	15.019	19.304	22.881
	Exact[17]	-	-	-	-	23.453
	Van[25]	5.321	9.809	15.064	19.339	22.912
	Ferreira et al. [10]	-	-	-	-	23.426
	Fiedler et al. [13]	-	-	-	-	23.043
	Liu [21]	5.401	9.985	15.374	19.537	23.154
	Chakrabart and Sheikh[4]	5.114	9.774	15.298	19.957	23.340
20	Present (12×12)	5.575	10.955	18.243	25.082	31.517
	Fiedler et al. [13]	-	-	-		31.529
50	Present (12×12)	5.678	11.359	19.418	27.392	35.278
	Fiedler et al. [13]	-	-	-	-	35.321
5	Present (12×12)	4.310	6.904	9.197	10.724	11.858
	Fiedler et al. [13]	-	-	-	-	11.601

$$\lambda cr = \lambda \frac{a^2}{E_2 h^3} \; 1 - Meshdivision$$

In the next example, the effect of number of layers and degree of orthotropy of individual layers on normalized uni-axial critical buckling load has been studied. The numbers of layers are varied from 3 to 5 and thickness ratio (a/h) is considered as 10 where h is the overall thickness of the plate. The material properties are taken same as in the previous section. The results are given in Table 3. It is to be noted that the present results are somewhat lesser than 3D elasticity solution of Noor [13] as compared to Fiedler et al. [33], Ferreira et al. [10] and Reddy and Phan[27] respectively. It has been observed in the previous example that the present finite element model based on higher order zigzag theory gives more accurate results compared to the results based on various other theories. It may be due to accurate modeling of the transverse shear deformation followed in the present finite element model to incorporate the exact flexible pattern of the structures. Due to inclusion of shear deformation in a refined manner the stiffness of the structure becomes less and therefore, the buckling load calculated by the present model gives lesser values than those obtained by other theories.

Table 3 Normalized critical uni-axial buckling loads (λ_{cr}) with various modular ratios for simply supported cross-ply square plate with thickness ratio (a/h = 10)

References	Laminate	E_1/E_2				
		3	10	20	30	40
Present (12×12)	0°/90°/0°	5.2284	9.6259	14.6458	18.6158	21.8527
3-D Elasticity [26]		5.3044	9.7621	15.0191	19.3040	22.8807
Ferreira et al. [10]		5.3869	9.8601	14.9746	19.0175	22.3070
Fiedler et al. [13]		5.3210	9.7180	14.7320	18.6902	21.9097
Reddy and Phan, HSDT [31]		5.3933	9.9406	15.2980	19.6740	22.3400
CLPT[13]		5.7538	11.4920	19.7120	27.9630	36.1600
Present (12×12)	0°/90°/0°/90°/0°	5.2750	9.8943	15.5177	20.2477	24.2896
3-D Elasticity [26]		5.3255	9.9603	15.6527	20.4663	24.5929
Ferreira et al. [12]		5.3552	10.0148	15.6805	20.4352	24.5024
Reddy and Phan, HSDT [31]		5.4096	10.1500	16.0080	20.9990	25.3080

$$\lambda cr = \lambda \frac{a^2}{E_2 h^3}$$

3.3 Cross-ply (0°/90°) laminate having different thickness ratio (a/h)

The effect of span to thickness ratio (a/h) on the uni-axial critical buckling load for simply supported two layer cross-ply (0°/90°) square plate is studied in this example. The material properties are same as in section 3.2 where E_1/E_2 is taken as 40. The results obtained by the present finite element model are shown in Table 4 along with those obtained by Van et al. [25], Reddy and Phan [27], and Chakrabarti and Sheikh [31] respectively. The same trend as explained before is also observed in the results presented in Table 4. The present results based on higher order zigzag theory are on the lower side compared to the results base on other theories as expected.

Table 4 Normalized critical uni-axial buckling loads (λ_{cr}) with various thickness ratios (a/h) for simply supported cross-ply [0°/90°] square plate

References	a/h			
	10	20	50	100
Present (12×12)	11.310	12.427	12.800	12.873
Van et al.[25]	11.360	12.551	12.906	13.039
Chakrabarti and Sheikh, FSDT [4]	11.349	12.510	12.879	12.934
Reddy and Phan, HSDT [31]	11.563	12.577	12.895	12.942

$$\lambda cr = \lambda \frac{a^2}{E_2 h^3}$$

3.4 Cross-ply (0°/90°/90°/0°) laminate having different aspect ratio (a/b)

In this example the effect of aspect ratio (a/b) on the uni-axial critical buckling load for simply supported four layer cross-ply (0°/90°/90°/0°) square plate is studied. The material properties are same as in the previous example. The results obtained by using the proposed model are shown in Table 5 along with those obtained by Fiedler et al. [13]. The results are in good agreement due the fact that the theory used in the present finite element model and in the

analytical approach adopted by Fiedler et al. [13] is nearly same. Some new results are also presented in Table 5.

Table 5 Normalized critical uni-axial buckling loads (λ_{cr}) with various aspect ratios (a/b) for simply supported cross-ply [0°/90°/90°/0°] square plate

a/b	References	a/h				
		5	10	20	50	100
0.5	Present (12×12)	8.739	18.347	25.746	29.087	29.657
1	Present (12×12)	11.858	23.134	31.517	35.278	35.923
	Fiedler et al. [13]	11.601	23.043	31.529	35.321	35.946
2	Present (12×12)	15.000	47.368	92.847	112.813	115.029

$$\lambda_{cr} = \lambda \frac{a^2}{E_2 h^3}$$

3.5 Effect of Different boundary conditions

The influence of different boundary conditions on normalized critical uni-axial buckling load ($\lambda_{cr} = \lambda \frac{a^2}{E_2 h_3}$) is investigated in the present section. The plate is considered simply supported (S) along the edges parallel to the y axis while the other edges have simply supported (S), clamped (C) or free (F) boundary conditions. The notation SSCF, for example refers to the simply supported boundary conditions of the two edges parallel to the y axis and the clamped and free conditions for the two edges parallel to the x axis. The eight layer $(0°/90°)_4$ square plate is analyzed with material properties same as in previous example while the thickness ratio (a/h) has been taken as 10 and 100. The normalized critical uni-axial buckling loads of the eight layer $(0°/90°)_4$ plate under different boundary conditions are shown in Table 6. All these results are presented for the first time.

Table 6 Normalized critical uni-axial buckling loads with different boundary conditions for cross-ply $[0°/90°]_4$ square plate

a/h	λ_{cr}			
	SSSS	SSSC	SSCC	CCCC
10	1.96	2.14	2.67	4.96
100	35.02	58.69	88.39	126.49

3.6 Cross-ply ($0^0/90^0/0^0$) laminate having different modular ratio (E_1/E_2) under bi-axial loading

The effect of modular ratio on normalized critical bi-axial buckling load ($\lambda_{cr} = \lambda \frac{a^2}{E_2 h_3}$) for simply supported cross-ply [0°/90°/0°] square plate with thickness ratio ($a/h = 10$) is studied in this example. The material properties are same as in section 3.2. The results obtained by the present element are shown in Table 7 along with other published results. The results obtained by the proposed finite element model agree reasonably well with the results obtained by Van et al., FSDT [25], Ferreira et al., FSDT[10] and Khedir and Librescu, HSDT[26] for lower E_1/E_2 however with higher value of this ratio i.e., with increased orthotrpic behavior

the present results are on the lower side as expected and as explained earlier. No pre-buckling state is considered since other results are also based on the same assumption.

Table 7 Normalized critical bi-axial buckling loads (λ_{cr}) with various modular ratios for simply supported cross-ply [0°/90°/0°] square plate with thickness ratio ($a/h = 10$)

References	E_1/E_2			
	10	20	30	40
Present (12×12)	4.812	7.320	8.688	9.784
Van et al. [25]	4.939	7.488	9.016	10.252
Ferreira et al. [10]	-	-	-	10.196
Fares and Zenkour [9]	4.963	7.588	8.575	10.202
Exact [17]	4.963	5.516	9.056	10.259

$$\lambda_{cr} = \lambda \frac{a^2}{E_2 h^3}$$

3.7 Anti-symmetric cross-ply (0°/90°/0°/90°) laminate

In the present example of anti-symmetric cross-ply (0°/90°/0°/90°) laminate (E_1/E_2 =40) firstly the effect of thickness ratio (a/h) on normalized critical ui-axial and bi-axial buckling load ($\lambda_{cr} = \lambda \frac{a^2}{E_2 h_3}$) with simply supported boundary conditions is studied. The material properties are same as in section 3.2. The comparison between the normalized critical ui-axial and bi-axial buckling load is shown in Figure 2. The comparison shows expected trend.

Next the effect of modular ratio (E_1/E_2) on normalized critical ui-axial and bi-axial buckling load ($\lambda_{cr} = \lambda \frac{a^2}{E_2 h_3}$) is studied with thickness ratio (a/h) = 10. The material properties are same as in section 3.1. The comparison between the normalized critical ui-axial and bi-axial buckling load is shown in Figure 3.

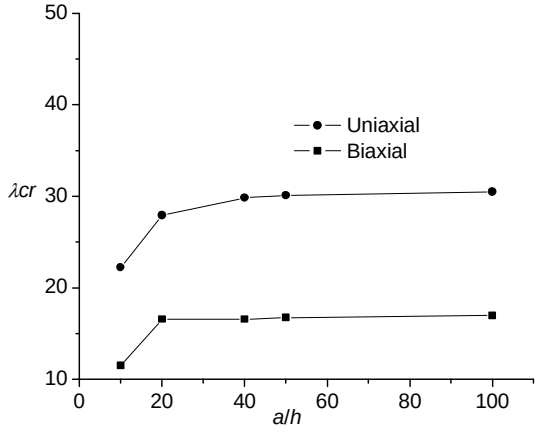

Figure 2 Comparison between normalized critical uniaxial and biaxial buckling load at different thickness ratio (a/h)

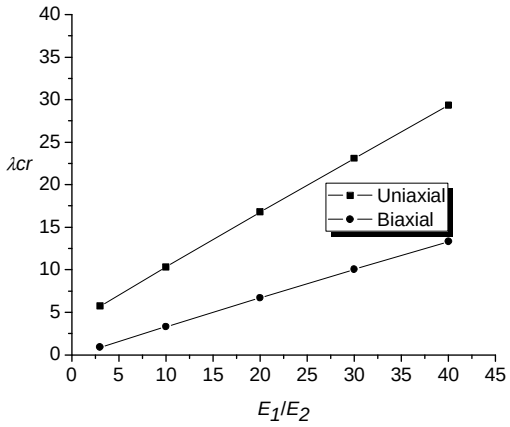

Figure 3 Comparison between normalized critical uniaxial and biaxial buckling load at different modular ratio (E_1/E_2)

3.8 Angle-ply (45°/-45°/-45°/45°) laminate having different thickness ratio (a/h)

In this section the effect of thickness ratio (a/h) on normalized critical pure shear buckling load ($\lambda_{cr} = \lambda \times 10^{-3}$) is studied taking E_1/E_2 =40 for an angle-ply (45°/-45°/-45°/45°) laminate with simply supported boundary conditions. The material properties are same as in section 3.2. The variation of the normalized critical pure shear buckling load with different thickness ratio (a/h) is shown in Figure 4.

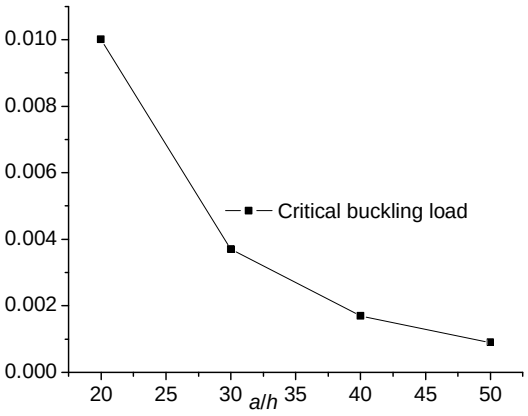

Figure 4 Variation of normalized critical shear buckling load with different thickness ratio (a/h)

4 CONCLUSIONS

In the present study, the buckling behaviour of laminated composite plates is studied using an efficient C^0 finite element model developed based on higher order zigzag theory. Many problems are solved covering different features of laminated composites such as boundary conditions, ply orientations aspect ratio, thickness ratio and loading etc. Numerical results

on buckling responses for different problems show that the proposed FE model for laminated composite plates is capable in predicting results very close to the exact solutions. Many new results are also generated. As such the model may be recommended for wide use in research and industrial applications.

References

[1] C.W. Bert and T.L.C. Chen. Effect of shear deformation on vibration of antisymmetric angle ply laminated rectangular plates. *Int. J. Solids Struct*, 14:465–473, 1978.

[2] K. Bhaskar and T.K. Varadan. Refinement of higher order laminated plate theories. *AIAA J*, 27:1830–1831, 1989.

[3] E. Carrera. Transverse normal stress effects in multilayered plates. *J. Appl. Mech*, 66:1004–1012, 1999.

[4] A. Chakrabarti and A.H. Sheikh. Buckling of laminated composite plates by a new element based on higher order shear deformation theory. *Mech. Composite Mater. Struct*, 10(4):303–317, 2003.

[5] A. Chakrabarti and A.H. Sheikh. A new triangular element to model inter-laminar shear stress continuous plate theory. *Int. J. Numer. Meth. Engg*, 60:1237–1257, 2004.

[6] A. Chakrabarti and A.H. Sheikh. Buckling of laminated sandwich plates subjected to partial edge compression. *Int. J.of Mech. sciences*, 47:418–436, 2005.

[7] M. Cho and R.R. Parmerter. An efficient higher order plate theory for laminated composites. *Compos. Struct*, 20:113–123, 1992.

[8] M. Cho and R.R. Parmerter. Efficient higher order composite plate theory for general lamination configurations. *AIAA J*, 31(7):1299–1306, 1993.

[9] M.E. Fares and A.M. Zenkour. Buckling and free vibration of non-homogeneous composite cross-ply laminated plates with various plate theories. *Compos. Struct*, 44:279–287, 1999.

[10] A.J.M. Ferreira, L.M. Castro, C.M.C. Roque, J.N. Reddy, and S. Bertoluzza. Buckling analysis of laminated plates by wavelets. *Comput. Struct*, 89:626–630, 2011.

[11] A.J.M. Ferreira, C.M.C. Roque, and P.A.L.S. Martins. Radial basis functions and higher order shear deformation theories in the analysis of laminated composite beams and plates. *Compos. Struct*, 66:287–293, 2004.

[12] A.J.M. Ferreira, C.M.C. Roque, A.M.A. Neves, R.M.N. Jorge, C.M.M. Soares, and K.M. Liew. Buckling and vibration analysis of isotropic and laminated plates by radial basis functions. *Composite Part B*, 42:592–606, 2011.

[13] L. Fiedler, W. Lacarbonara, and F. Vestroni. A generalized higher-order theory for buckling of thick multi-layered composite plates with normal and transverse shear strains. *Compos. Struct*, 92:3011–3019, 2010.

[14] M. Ganapathi, Amit Kalyani, Bhaskar Mondal, and T. Prakash. Free vibration analysis of simply supported composite laminated panels. *Compos. Struct*, 90:100–103, 2009.

[15] M. Ganapathi and D.P. Makhecha. Free vibration analysis of multi-layered composite laminates based on an accurate higher-order theory. *Composites: Part B*, 32:535–543, 2001.

[16] T. Kant and K. Swaminathan. Free vibration of isotropic, orthotropic, and multilayer plates based on higher order refined theories. *J. Sound Vib*, 24:319–327, 2001.

[17] A.A. Khdeir and L. Librescu. Analysis of symmetric cross-ply elastic plates using a higher-order theory. part ii: Buckling and free vibration. *Compos. Struct*, 9:259–277, 1988.

[18] J. Lee. Thermally induced buckling of laminated composites by a layer-wise theory. *Comput Struct*, 65:917–922, 1997.

[19] X.Y Li and Z. Liu. Generalized laminate theories based on double superposition hypothesis. *Int. J. Numer. Methods Engg*, 40:1197–1212, 1997.

[20] D. Liu and X. Li. An overall view of laminate theories based on displacement hypothesis. *J. Compos. Mater*, 30:1539–1561, 1996.

[21] L. Liu, L.P. Chua, and D.N. Ghista. Mesh-free radial basis function method for static, free vibration and buckling analysis of shear deformable composite laminates. *Compos. Struct*, 78:58–69, 2007.

[22] Bhaskar Mondal, M. Ganapathi, and Amit Kalyani. On the elastic stability of simply supported anisotropic sandwich panels. *Compos. Struct*, 80:631–635, 2007.

[23] H. Murakami. Laminated composite plate theory with improved in-plane responses. *J. Appl. Mech*, 53:661666, 196.

[24] P. Nali, E. Carrera, and S. Lecca. Assessments of refined theories for buckling analysis of laminated plates. *Compos. Struct*, 93(2):456464, 2011.

[25] H. Nguyen-Van, N. Mai-Duy, W. Karunasena, and T. Tran-Cong. Buckling and vibration analysis of laminated composite plate/shell structures via a smoothed flat shell element with in-plane rotations. *Compos. Struct*, 89:612–625, 2011.

[26] A.K. Noor. Stability of multilayered composite plates. *Fibre Sci. Technol*, 8(2):81–89, 1975.

[27] N.D. Phan and J.N. Reddy. Analyses of laminated composite plates using a higher-order shear deformation theory. *Int. J. Numer. Methods Engg*, 21:2201–2219, 1985.

[28] J.N. Reddy. Free vibration of antisymmetric angle-ply laminated plates including transverse shear deformation by the finite element method. *J. Sound Vib*, 4:565–576, 1979.

[29] J.N. Reddy. *Cellular solids: structures & properties*. CRC Press, Boca Raton, FL, 2nd ed edition, 2004.

[30] J.N Reddy and N.D. Phan. Stability and vibration of isotropic, orthotropic and laminated plates according to a higher-order shear deformation theory. *J. Sound Vib*, 98:157–170, 1985.

[31] J.N. Reddy and N.D. Phan. Stability and vibration of isotropic, orthotropic and laminated plates according to a higher-order shear deformation theory. *J. Sound Vibr*, 98(2):157–170, 1985.

[32] E. Reissner and Y. Stavasky. Bending and stretching of certain types of aelotropic elastic plates. *J. Appl. Mech*, 28:402–408, 1961.

[33] D. Cook Robert, S. Malkus David, E. Michael Plesha, and J. Witt Robert. *Concepts and Applications of Finite Element Analysis*. John Wiley & Sons Pte. Ltd, 4th edition edition, 2003.

[34] M. Di Sciuva. A refined transverse shear deformation theory for multilayered anisotropic plates. *Atti. Academia Scienze Torino*, 118:279–295, 1984.

[35] M. Di Scuiva. Multilayered anisotropic plate models with continuous interlaminar stress. *Comput. Struct*, 22(3):149167, 1992.

[36] A.H. Sheikh and A. Chakrabarti. A new plate bending element based on higher order shear deformation theory for the analysis of composite plates. *Finite Element Anal Des*, 39:883–903, 2003.

[37] I. Shufrin, O. Rabinovitch, and M. Eisenberger. Buckling of symmetrically laminated rectangular plates with general boundary conditions a semi analytical approach. *Compos. Struct*, 82:521–531, 2008.

[38] P. Sundaresan, G. Singh, and G.V. Rao. Buckling of moderately thick rectangular composite plates subjected to partial edge compression. *International Journal of Mechanical Sciences*, 40(11):1105–1117, 1998.

[39] W. Zhen and C. Wanji. Free vibration of laminated composite and sandwich plates using global-local higher-order theory. *J. Sound Vib*, 298:333–349, 2006.

[40] W. Zhen and C. Wanji. Buckling analysis of angle-ply composite and sandwich plates by combination of geometric stiffness matrix. *Comput. Mech*, 39:839–848, 2007.